FERMILAB-PUB-14-426-APC
Submitted to Phys. Rev. ST Accel. Beams

Transverse Mode Coupling Instability with chromaticity and space charge

V. Balbekov

Fermi National Accelerator Laboratory

P.O. Box 500, Batavia, Illinois 60510[*]

(Dated: October 29, 2014)

Abstract

Transverse mode coupling instability is considered in the paper at different bunch and wake shapes. Exact solution for "hollow" bunch is arrived at and used to develop a proper technique for more realistic distributions. The three-modes approach is proposed for arbitrary bunch with chromaticity included. It is shown that the TMCI threshold and rate depend only slightly on the bunch model used being rather sensitive to the wake shape. Resistive wall wake is considered in detail, and a comparison of the TMCI and collective mode instability with this wake is performed. Space charge tune shift of arbitrary value is included in the consideration providing a firm bridge between the known cases of absent and dominating space charge.

PACS numbers: 29.27.Bd

[*]Electronic address: `balbekov@fnal.gov`

Operated by Fermi Research Alliance, LLC under Contract No. De-AC02-07CH11359 with the United States Department of Energy.

I. INTRODUCTION

Transverse Mode Coupling Instability of a single bunch in a circular accelerator, also known as "fast head-tail instability" or "head-tail turbulence", has been considered first by R. D. Kohaupt who used a simple model of two particles propelling each other through the mediation of constant wake fields [1]. Later the TMCI theory has been developed on the base of Vlasov equation [2, 3]. The instability has been treated as a result of reciprocal influence of a neighboring pair of head-tail modes which frequencies approach each other due to the wake field (two-modes model). Effect of the beam space charge has been investigated later in papers [4–6].

However, there is a number of unresolved problems in this area including reliability of the two-modes model, role of chromaticity, dependence of the effect on the bunch and wake shape. The space charge investigations look incomplete being based either on not quite realistic models [4] or restricted to ultimate cases only [5, 6].

These and other problems are considered in presented paper where a unified three-modes model is proposed and used far and wide. The model itself is built on the base of exact analytical solution which has been found with hollow bunch model without any additional assumptions. It is shown that the TMCI depends only slightly on the bunch shape but is rather sensitive to the wake shape. Resistive wall wake is investigated especially to assign which effect is more danger in specific cases: either TMCI or collective mode instability which is unavoidable with the long-range wake. Chromaticity is included to demonstrate that there is no the well defined boundary between the head-tail instability (separated multipoles) and TMCI (coalesced multipoles). Space charge influence is investigated with arbitrary ratio of betatron tune shift to synchrotron tune.

II. BASIC EQUATIONS AND DEFINITIONS [6]

Linear synchrotron oscillations are considered in this paper. They are characterized by amplitude A and phase ϕ or by corresponding Cartesian coordinates:

$$\theta = A\cos\phi, \qquad u = A\sin\phi. \tag{1}$$

So θ is azimuthal deviation of a particle from the bunch center in the rest frame whereas the variable u is proportional to the momentum deviation with respect to the central bunch

momentum (proportionality coefficient is not a factor in this paper).

Steady state of a bunch will be described by distribution function $F(A)$ and by corresponding linear density

$$\rho(\theta) = \int_{-\infty}^{\infty} F(\sqrt{\theta^2 + u^2})\, du \tag{2}$$

with the normalization conditions

$$2\pi \int_0^{\infty} F(A)\, AdA = 1, \qquad \int_{-\infty}^{\infty} \rho(\theta)\, d\theta = 1. \tag{3}$$

Coherent transverse displacement of the bunch dependent on time and position in the longitudinal phase space will be described by the function

$$Y(A, \phi) \exp\big[- i(Q_0 + \zeta)\, \theta - i\, (Q_0 + \nu)\, \Omega_0 t \big] \tag{4}$$

where Ω_0 is the revolution frequency, Q_0 is the central betatron tune, ν is an addition to the coherent tune caused by the wake field, and ζ is the normalized chromaticity:

$$\zeta = \frac{\Omega_0 Q'_p}{\Omega'_p} = \frac{\xi}{1/\gamma^2 - \alpha}, \tag{5}$$

with ξ as usual chromaticity, and α as the momentum compaction factor. As it has been shown in Ref. [6], the function Y satisfies the equation

$$\nu Y + i\, Q_s \frac{\partial Y}{\partial \phi} = 2 \int_{\theta}^{\infty} q(\theta' - \theta) \exp\big[i(\zeta - \nu)(\theta - \theta') \big] d\theta' \int_{-\infty}^{\infty} F(A') Y(A', \phi')\, du' \tag{6}$$

where Q_s is synchrotron tune, and $q(\theta)$ is the reduced wake function which is related to the usual wake field function $W_1(z)$ by the equation:

$$q(\theta) = \frac{r_0 R N W_1(R\theta)}{8\pi\beta\gamma Q_0} \tag{7}$$

with $r_0 = e^2/mc^2$ as classic radius of the particle, R as the accelerator radius, N as the bunch population, β and γ as normalized velocity and energy.

It is assumed that $q(\theta)$ is rather short range function so that the wake field cannot reach neighboring bunches or turns. With this reservation, constant wake $q = q_0$ will be used to start with, and more general case will be considered in Sec. 6. Eq. (6) with this wake obtains the form

$$\nu Y + i\, Q_s \frac{\partial Y}{\partial \phi} = 2 q_0 \exp(i\zeta_\nu \theta) \int_{\theta}^{\infty} \exp(-i\zeta_\nu \theta') d\theta' \int_{-\infty}^{\infty} F(A') Y(A', \phi')\, du' \tag{8}$$

where $\zeta_\nu = \zeta - \nu$. Note that, in most cases, the addition ν is rather small to identify ζ_ν with normalized chromaticity given by Eq. (5).

III. EXACT SOLUTION FOR HOLLOW BUNCH (CONSTANT WAKE, NO CHROMATICITY)

The hollow bunch model which is applied in this section is characterized by the functions

$$F(A) = \frac{\delta(A - A_0)}{2\pi}, \qquad \rho(\tau) = \frac{1}{\pi\sqrt{\theta_0^2 - \theta^2}} \tag{9}$$

where $A_0 = \theta_0$ is synchrotron amplitude of any particle and, simultaneously, the bunch half-length. The case $\zeta_\nu = 0$ will be considered in detail what means zero chromaticity, in practice. Special interest of this case is that its exact solution can be obtained without any additional assumptions. Therefore the results can be substantially used further for development of adequate approximate methods applicable for more realistic models.

The only amplitude $A = A_0$ is essential in this case. Therefore Eq. (8) can be reduced to the one-dimension equation for the function $Y(\phi) \equiv Y(A_0, \phi)$:

$$\nu Y(\phi) + i\, Q_s Y'(\phi) = \frac{q_0}{\pi} \int_{-[\phi]}^{[\phi]} Y(\phi')\, d\phi' \tag{10}$$

where $[\phi]$ is the periodic polygonal function of period 2π taking the value $[\phi] = |\phi|$ at $|\phi| < \pi$. It is convenient to separate even and odd parts of the function $Y(\phi)$ presenting it in the form $Y(\phi) = Y_+(\phi) + Y_-(\phi)$, with $Y_+(\phi) = Y_+(-\phi)$, and $Y_-(\phi) = -Y_-(-\phi)$. It is easy to see that the even part satisfies the equation

$$Q_s^2 Y_+''(\phi) + \nu^2 Y_+(\phi) = \frac{2q_0\nu}{\pi} \int_0^{[\phi]} Y_+(\phi') d\phi' \tag{11}$$

Restricting the consideration to the region $0 < \phi < \pi$, one can transform it to ordinary third order differential equation

$$Y_+'''(\phi) + \frac{\nu^2}{Q_s^2} Y_+'(\phi) = \frac{2q_0\nu}{\pi Q_s^2} Y_+(\phi) \tag{12}$$

with boundary conditions

$$Y_+'(0) = 0, \quad Q_s^2 Y_+''(0) + \nu^2 Y_+(0) = 0, \quad Y_+'(\pi) = 0. \tag{13}$$

General solution of this equation is

$$Y_+(\phi) = \sum_{j=1}^{3} C_j \exp\left(\frac{\nu\lambda_j}{Q_s}\right) \tag{14}$$

where λ_{1-3} are roots of the third order algebraic equation:

$$\lambda^3 + \lambda = g, \qquad g = \frac{2q_0 Q_s}{\pi\nu^2} \tag{15}$$

and C_{1-3} are some constant which have to be determined trough the boundary conditions. The substitution of Eq. (14) to (13) provides a system of linear uniform equation for C_{1-3} which is solvable if its determinant is 0. It results in the dispersion equation for the bunch eigentunes ν:

$$\begin{aligned} &\lambda_1(\lambda_2 - \lambda_3)(1 - \lambda_2\lambda_3)\exp(\pi\nu\lambda_1/Q_s) \quad + \\ &\lambda_2(\lambda_3 - \lambda_1)(1 - \lambda_3\lambda_1)\exp(\pi\nu\lambda_2/Q_s) \quad + \\ &\lambda_3(\lambda_1 - \lambda_2)(1 - \lambda_1\lambda_2)\exp(\pi\nu\lambda_3/Q_s) = 0 \end{aligned} \tag{16}$$

Therefore following steps are evident for handling the problem: (i) to find the roots λ_{1-3} of first Eq. (15) with given parameter g; (ii) to use them in Eq. (16) for determination of possible solutions ν; (iii) to substitute the solution in second Eq. (15) obtaining dependence $\nu(q_0)$ by exclusion of parameter g.

Generally, this way is applicable for all roots including complex ones. However, in this section we will restrict our consideration to real rots only, postponing discussing of complex eigentunes to next sections where they will be analyzed with chromaticity taken into account.

Eq. (16) gas infinite number of solutions, and some of them are plotted in Fig. 1. It is seen that $\nu \simeq mQ_s$ at small q_0 which case has to be treated as independent oscillations of different multipoles. These tunes are real numbers that is instability is impossible at slight wake and zero chromaticity. Complex roots appear for the first time at $|q_0| > 0.567\,Q_s$ as a result of coalescing of the multipoles $m = 0$ and $m = \pm 1$, dependent on sign of the wake. Presented inequality should be treated as the threshold of the lowest TMCI mode. Higher TMCI modes are possible too being caused by a coalescence of higher multipoles. They have essentially higher thresholds as it is shown in Table I (only positive wakes are considered in the Table; negative wakes create similar pattern with negative multipoles). No other coalescences and TMCI appearances have been observed at the calculations.

Because thresholds of the higher TMCI modes are relatively high, they are not so interesting in practice, and will be not considered in subsequent sections of the paper.

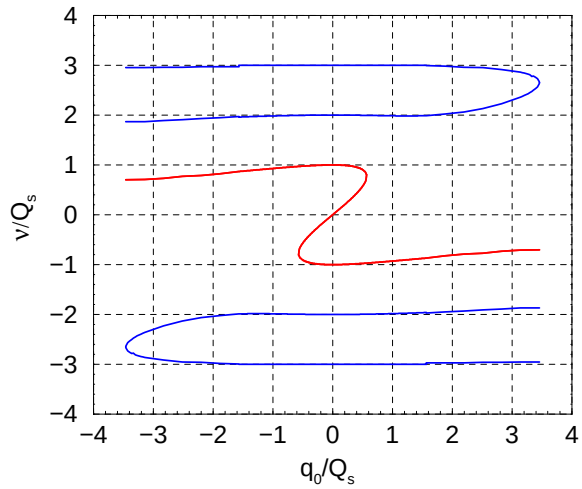

FIG. 1: Real eigentunes of hollow bunch without chromaticity (exact solutions). There are complex roots at $|q_0|/Q_s > 0.567$ (not shown).

TABLE I: Threshold of different TMCI modes

Coalesced multipoles	(0-1)	(2-3)	(4-5)	(6-7)	(8-9)	(10-11)
$(q_0)_{thresh}/Q_s$	0.567	3.459	7.366	11.894	16.871	22.198

IV. INTEGRAL EQUATION FOR REALISTIC DISTRIBUTIONS (CONSTANT WAKE, NO CHROMATICITY)

General solution of Eq. (8) can be presented as a Fourier series:

$$Y(A,\phi) = \sum_m Y_m(A)\exp(im\phi) \tag{17}$$

which is just expansion over the multipoles. Its substitution to Eq. (8) allows to get set of coupled integral equations for the functions $Y_m(A)$:

$$(\nu - mQ_s)\,Y_m(A) = \; 2\pi q_0 \sum_n \int_0^\infty K_{m,n}(A,A')Y_n(A')\,F(A')A'\,dA' \tag{18}$$

with the kernels

$$K_{m,n}(A,A') = \frac{2}{\pi^2}\int_{-A}^{A}\exp(i\zeta_\nu\theta)\,\frac{T_m(\theta/A)\,d\theta}{\sqrt{A^2-\theta^2}}\int_{\theta_{A'}}^{A'}\exp(-i\zeta_\nu\theta')\,\frac{T_n(\theta'/A')\,d\theta'}{\sqrt{A'^2-\theta'^2}} \tag{19}$$

where $T_m(x) = \cos(m \arccos x)$ are Chebyshev polynomials,

$$\theta_{A'} = \theta \ \text{ at } \ A'^2 > \theta^2, \ \text{ and } \ \theta_{A'} = A'\theta/|\theta| \ \text{ at } \ A'^2 < \theta^2.$$

Chromaticity is included in the expression for future but actually it is not considered in this section.

As is evident from Fig. 1, only 3 multipoles are essentially involved in the formation of the lowest TMCI mode whereas the multipoles $|m| \geq 2$ remain almost untouched and can be neglected. Following features of the kernels are important at the consideration being valid at $\zeta_\nu = 0$.

$$K_{m,m}(A, A') = K_{m,-m}(A, A') = \delta_{m,0} \quad (\text{any } m) \tag{20}$$

$$K_{0,\pm1}(A, A') = -K_{\pm1,0}(A', A) = \frac{2}{\pi^2 A'} \int_{-A}^{A} \sqrt{\frac{A'^2 - \theta_{A'}^2}{A^2 - \theta^2}}\, d\theta \tag{21}$$

Therefore equations for three mentioned multipoles can be written as

$$\nu Y_0(A) = 2\pi q_0 \int_0^\infty \Big\{ Y_0(A') + K_{0,1}(A, A')\big[Y_{-1}(A') + Y_1(A')\big] \Big\} F(A') A'\, dA' \tag{22a}$$

$$(\nu \mp Q_s) Y_{\pm1}(A) = -2\pi q_0 \int_0^\infty K_{0,1}(A', A) Y_0(A') F(A') A'\, dA' \tag{22b}$$

Excluding $Y_{\pm1}$ one can arrive at the ordinary integral equation for the function $Y_0(A)$:

$$\nu Y_0(A) = 2\pi q_0 \int_0^\infty Y_0(A') F(A') A'\, dA' - \frac{8\pi^2 q_0^2 \nu}{\nu^2 - Q_s^2} \int_0^\infty \mathbf{K}(A, A') Y_0(A') F(A') A'\, dA' \tag{23}$$

with the kernel

$$\mathbf{K}(A, A') = \int_0^\infty K_{0,1}(A, X) K_{0,1}(A', X) F(X)\, X dX \tag{24}$$

Multiplying Eq. (23) by $Y_0(A)F(A)A$ and integrating over A, one can get a simple equation for ν

$$\frac{\nu - q_{ef}}{2}\left(\nu - \frac{Q_s^2}{\nu}\right) = -\alpha^2 q_0^2 \tag{25}$$

with the coefficients

$$q_{ef} = \frac{2\pi q_0 \left[\int_0^\infty Y_0(A) F(A)\, A dA\right]^2}{\int_0^\infty Y_0^2(A) F(A) A\, dA} \tag{26}$$

and

$$\alpha^2 = \frac{4\pi^2 \int_0^\infty \int_0^\infty \mathbf{K}(A, A')\, Y_0(A) Y_0(A')\, F(A) F(A')\, AA'\, dA dA'}{\int_0^\infty Y_0^2(A) F(A) A\, dA} \tag{27}$$

Solution of Eq. (25) allows to know all characteristics of the lowest TMCI mode of arbitrary bunch, including its threshold and rate. Of course, it is pithy if the function $Y_0(A)$ is known being at least an approximate solution of Eq. (23). The simplest and very reasonable choice is $Y_0 = 1$ because it coincides with solution without coupling and is in a full agreement with special case of hollow bunch. Then $q_{ef} = q_0$, and Eq. (27) also obtains the compact form (see Appendix):

$$\alpha^2 = \frac{8}{\pi}\int_0^\infty F(A)A^3\,dA\,\Big[\int_0^\pi \rho(A\cos\phi)\sin^2\phi\,d\phi\Big]^2 \tag{28}$$

Results of calculations by this formula are collected in Table II for several distributions including hollow, rectangular, parabolic, and Gaussian bunches. The TMCI thresholds are also shown in the Table being found by solution of Eq. (25) with obtained α^2 and presented as $Thresh = |q_0|_{thresh}/Q_s$. Results of Sec. 3 for hollow bunch are added in this line and marked as Hollow*.

TABLE II: TMCI threshold of different bunch shapes

	Hollow*	Hollow	Rectang	Parabol	Gauss
α^2	N/A	$16/\pi^4$	1/6	93/560	0.16163
$Thresh$	0.5671	0.5689	0.5672	0.5676	0.5708
$1/(1+2\alpha)$	N/A	0.552	0.551	0.551	0.554

Note that rather precise expression for the threshold can be found with neglect of reciprocal influence of multipoles $m = \pm 1$ which formally means the approximation $(\nu^2 - Q_s^2)/2\nu \simeq \nu - sQ_s$ with s as q_0 sign. The TMCI tunes and threshold are in this approximation

$$\nu \simeq \frac{q_0 + Q_s}{2} \pm \sqrt{\left(\frac{q_0 - Q_s}{2}\right)^2 - q_0^2\alpha^2}, \tag{29}$$

$$Thresh = \frac{|q_0|_{thresh}}{Q_s} = \frac{1}{1+2\alpha} \simeq 0.55 \tag{30}$$

Corresponding row is added to Table II to demonstrate that associated underestimation of the threshold does not exceed 3%.

Global picture is shown in Fig. 2 where complex roots of Eq. (25) are plotted against the wake strength. Data of previous section are also included in the plot being transfered from

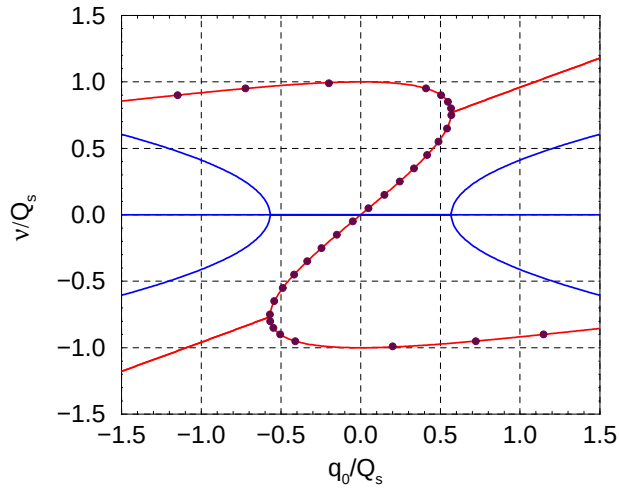

FIG. 2: Eigentunes of hollow bunch without chromaticity (3-modes approximation). Red and blue curves present real and imaginary parts of the tune. Solid lines are obtained by solution of Eq. (25), and some data are transfered from Fig. 1 being presented by circles.

Fig. 1 and presented by dark circles. Note that 2-modes approximation gives an error 3-5% but fully ignores the arms of the red curve where sign ν is opposite of the wake sign.

Two points stand out at once. First, results of this 3-modes method are in ideal agreement with exact solution of Eq. (10) for hollow bunch when all multipoles are taken into account. Second not so expected result appears as very weak dependence of the tunes on the bunch shape. It is seen from Table 2 that even the models so far apart as hollow and Gaussian bunches lead to practically indistinguishable results. Therefore it would serve no purpose to ask which bunch shape has been applied to plot the curve in Fig. 2. Further still, rather close value $Thresh = 2/\pi \simeq 0.64$ has been obtained with 2-particles model developed in the original paper [1]. Thus it would be valid to say that the lowest TMCI threshold with rectangular wake in usual terms is

$$\frac{r_0 R N |W_1|}{8\pi\beta\gamma Q_0 Q_s} > 0.57$$

independently on the bunch shape.

V. INSTABILITY RATE WITH CHROMATICITY (CONSTANT WAKE)

Next step is an invoking of chromaticity to consider its influence on the instability growth rate. It could be done by taking into account corresponding exponential factors in the kernels given by Eq. (19). However, this way would lead to rather unwieldy expressions, so we will apply slightly modified method using a simplified version of the 3-modes approximation It will be seen in the end that cost of this simplification is no more than 3% of accuracy.

It follows from Eq. (21) and (22b) that, with approximation $Y_0 = 1$, other involved modes are

$$Y_{\pm 1}(A) \propto A \int_0^{\pi} \rho(A\cos\phi)\sin^2\phi\, d\phi \tag{31}$$

This expression is not too far removed from $Y_{\pm 1} \propto A$ for all considered distributions providing exact result for the rectangular bunch. It means that above used 3-modes solution is reasonably close to the function

$$Y(A,\phi) = 1 + C_\theta\theta + C_u u \tag{32}$$

with C_θ and C_u as some unknown constants. This statement will be actually monitored below, though the main goal of this section is an incorporation of TMCI and head-tail instabilities.

It is pertinent to note at this point that only lowest radial head-tail modes are actually involved in Eq. (32). It was an immaterial factor in previous consideration because the higher radial modes were absent in those cases at all. However, they come to realistic distributions with chromaticity which circumstance should be discussed now.

The main thing is that dependence of the higher modes on intensity and wake strength is relatively slight effect which is proportional to chromaticity. Therefore, though their merging and resulting TMCI is possible in principle, it would have significantly higher threshold being probably inessential in practice (see e.g. [3]). At least, it is quite allowably to ignore the higher head-tail modes when the lowest TMCI mode is the subject of interest.

Substitution of the intended solution given by Eq. (32) to Eq. (8) leads to the expression

$$\nu + (\nu C_\theta + iQ_s C_u)\,\theta + (\nu C_u - iQ_s C_\theta)\,u = 2q_0 \exp(i\zeta\theta) \int_\theta^\infty \rho(\theta')(1+C_\theta\theta')\exp(-i\zeta\theta')\, d\theta' \tag{33}$$

Relation $C_u = iC_\theta Q_s/\nu$ follows from this immediately. Two more equations are achievable

through the multiplication of Eq. (33) by $\rho(\theta)$ or $\rho(\theta)\theta$ with subsequent integration over θ:

$$\nu - 2q_0 \int_{-\infty}^{\infty} \rho(\theta) \exp(i\zeta\theta) d\theta \int_{\theta}^{\infty} \rho(\theta') \exp(-i\zeta\theta') d\theta'$$
$$= 2q_0 C_\theta \int_{-\infty}^{\infty} \rho(\theta) \exp(i\zeta\theta) d\theta \int_{\theta}^{\infty} \rho(\theta')\theta' \exp(-i\zeta\theta') d\theta' \tag{34a}$$

$$C_\theta \left(\frac{\nu^2 - Q_s^2}{\nu} - 2q_0 \int_{-\infty}^{\infty} \rho(\theta) \exp(i\zeta\theta)\, \theta d\theta \int_{\theta}^{\infty} \rho(\theta') \exp(-i\zeta\theta')\, \theta' d\theta' \right)$$
$$= -2q_0 \int_{-\infty}^{\infty} \rho(\theta) \exp(i\zeta\theta)\, d\theta \int_{\theta}^{\infty} \rho(\theta')\theta' \exp(-i\zeta\theta')\, d\theta' \tag{34b}$$

Dispersion equation for tune ν is derived from these relations by excluding of parameter C_θ. To avoid a cumber, we restrict the consideration by the case $|\zeta\theta_0| \ll 1$ which assumption leads to the equation

$$(\nu - q_0 + i\alpha q_0 \chi) \left(\frac{\nu^2 - Q_s^2}{2\nu} - i\beta q_0 \chi \right) = -q_0^2 \left(\alpha - \frac{i\chi}{4} \right)^2 \tag{35}$$

where $\chi = 2\sqrt{2}\, \zeta_\nu \sigma_\theta$, and following designations are used:

$$\sigma_\theta^2 = \int_{-\infty}^{\infty} \rho(\theta)\, \theta^2 d\theta \tag{36a}$$

$$\alpha = \frac{\sqrt{2}}{\sigma_\theta} \int_{-\infty}^{\infty} \rho(\theta)\, \theta d\theta \int_{0}^{\theta} \rho(\theta')\, d\theta' \tag{36b}$$

$$\beta = \frac{1}{\sigma_\theta^3 \sqrt{2}} \int_{-1}^{1} \rho(\theta)\, \theta d\theta \int_{0}^{\theta} \rho(\theta')\, \theta'^2 d\theta' \tag{36c}$$

Because σ_θ is rms bunch length, χ can be treated as betatron phase advance caused by

TABLE III: TMCI coefficients of different bunches

	Hollow	Boxcar	Parabolic	Gaussian
σ_θ^2	$\theta_0^2/2$	$\theta_0^2/3$	$\theta_0^2/5$	Any
α	0.405	0.408	0.407	0.400
α^2	0.164	0.167	0.166	0.160
β	0.135	0.123	0.113	0.100

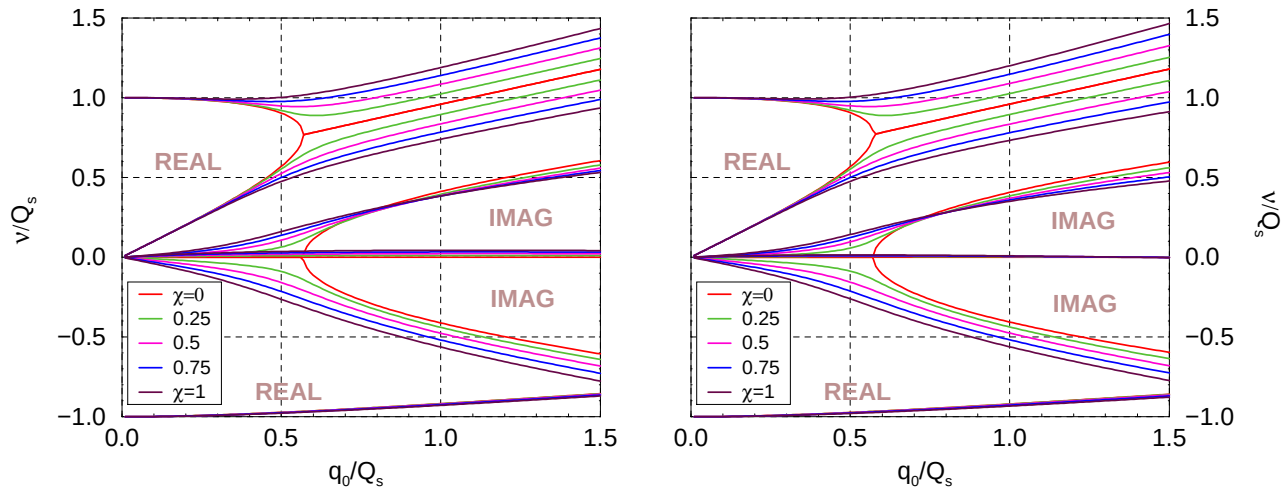

FIG. 3: Eigentunes with chromaticity: left – hollow bunch, right – Gaussian distribution. All the curves are odd functions of the wake strength. Real parts do not depend on sign of chromaticity, imaginary parts change sign. Some curves are indistinguishable because the modes starting from the point $\nu = -Q_s$ almost do not depend on chromaticity.

chromaticity in the entire bunch (it is really true for the hollow bunch of length $2\theta_0$ when $\sigma_\theta = \theta_0/\sqrt{2}$). Other parameters are presented in Table III for several distributions. It is seen that, at $\chi = 0$, Eq. (35) coincides with Eq. (25) not only formally but also actually, because the discrepancy of coefficients α^2 does not exceed 1%. Parameters β associated with chromaticity depends on distribution a bit stronger but moderately.

Complex solutions of Eq. (35) are plotted in Fig. 3 for hollow and Gaussian bunches. Only positive wakes and chromaticities are presented in the graphs because all curves have following symmetry properties: (i) they are odd functions of q_0/Q_s; (ii) the real parts of the tunes do not depend on sign of chromaticity; (iii) the imaginary additions reflect specularly with respect to the line $\nu = 0$ when the chromaticity change sign. Comparison of the figures suggest again that the TMCI with chromaticity depends of the bunch shape very weakly when rms bunch length is fixed.

A reasonable accuracy can be reached also with 2-modes approximation which has been used earlier for Eq. (29)

$$\nu \simeq \frac{q_0 + Q_s - iq_0\chi(\alpha - \beta)}{2} \pm \sqrt{\left(\frac{q_0 - Q_s - iq_0\chi(\alpha + \beta)}{2}\right)^2 - q_0^2\left(\alpha - \frac{i\chi}{4}\right)^2} \qquad (37)$$

The instability has no threshold with chromaticity, and TMCI appears against the head-tail

background. In particular, it is seen from Fig. 3 that the TMCI and head-tail contributions are comparable at $|q_0| \simeq 0.7\,Q_s$ and $|\theta_0\zeta| \simeq 0.5$. However, the transverse mode coupling is negligible at all at $|q_0| \ll Q_s$ when the separate multipole approximation is applicable, and the known expression for eigentunes of hollow bunch follows from Eq. (17)-(19) being valid with any integer m

$$\nu_m = mQ_s + q_0\delta_{m,0} + \frac{8iq_0\theta_0\zeta_\nu}{\pi^2(4m^2-1)}$$

VI. REALISTIC BUNCH WITH ARBITRARY WAKE (NO CHROMATICITY)

It would be beyond reason to treat the rectangular wake as an exclusive case. On the contrary, Eq. (31) can be applied as an approximate solution of general Eq. (6) to look for the TMCI parameters with arbitrary wake function. Then the same as above transformations result in the dispersion equation like Eq. (25)

$$(\nu - q_{ef})\left(\frac{\nu^2 - Q_s^2}{2\nu} - \alpha_2 q_{ef}\right) = -\alpha_1^2 q_{ef}^2 \tag{38}$$

with the coefficients

$$q_{ef} = 2\int_0^\infty \tilde{q}(\theta)d\theta \times \int_{-\infty}^\infty \rho(\theta' - \theta/2)\;\;\rho(\theta' + \theta/2)\,d\theta' \tag{39a}$$

$$\alpha_1 = \frac{1}{\sigma_\theta q_{ef}\sqrt{2}}\int_0^\infty \tilde{q}(\theta)\,\theta d\theta \times \int_{-\infty}^\infty \rho(\theta' - \theta/2)\,\rho(\theta' + \theta/2)\,d\theta' \tag{39b}$$

$$\alpha_2 = \frac{1}{\sigma_\theta^2 q_{ef}}\int_0^\infty \tilde{q}(\theta)\,d\theta \int_{-\infty}^\infty \rho(\theta' - \theta/2)\,\rho(\theta' + \theta/2)\,(\theta'^2 - \theta^2/4)\,d\theta' \tag{39c}$$

where σ_θ is rms bunch length given by Eq. (36a). Note that chromaticity could be included in the consideration because $\tilde{q}(\theta) = q(\theta)\exp(-i\zeta_\nu\theta)$. However, we will investigate in this section only the case $\zeta_\nu = 0,\ \tilde{q} = q$. Besides, we restrict ourself to 2-modes approximation as it was introduced for Eq. (29). Then solutions of dispersion equation (38) are

$$\nu \simeq \frac{q_{ef}(1+\alpha_2) + sQ_s}{2} \pm \sqrt{\left[\frac{q_{ef}(1-\alpha_2) - sQ_s}{2}\right]^2 - \alpha_1^2 q_{ef}^2} \tag{40}$$

Without chromaticity, α_{1-2} are real numbers not depending on q_{ef}. Therefore the TMCI threshold is in this case

$$|q_{ef}|_{thresh} = \frac{Q_s}{1+2\alpha}, \qquad \alpha = \alpha_1 - \frac{\alpha_2}{2} \tag{41}$$

For Gaussian bunch with dispersion σ_θ, used parameters obtain the forms

$$q_{ef} = \frac{1}{\sigma_\theta \sqrt{\pi}} \int_0^\infty \exp\left(-\frac{\theta^2}{4\sigma_\theta^2}\right) q(\theta)\, d\theta \tag{42a}$$

$$\alpha_1 = \frac{1}{2\sqrt{2\pi}\, \sigma_\theta^2 q_{ef}} \int_0^\infty \exp\left(-\frac{\theta^2}{4\sigma_\theta^2}\right) q(\theta)\, \theta d\theta \tag{42b}$$

$$\alpha_2 = \frac{1}{4\sqrt{\pi}\, \sigma_\theta q_{ef}} \int_0^\infty \left(1 - \frac{\theta^2}{2\sigma_\theta^2}\right) \exp\left(-\frac{\theta^2}{4\sigma_\theta^2}\right) q(\theta)\, d\theta \tag{42c}$$

Two examples are considered below.

A. Short rectangular wake

Gaussian bunch with a rectangular wake of restricted length θ_w is considered in this subsection as first example. Eq. (42) gives in this case

$$q_{ef} = q_0 \,\mathrm{erf}(x), \quad \alpha_1 = \frac{1 - \exp(-x^2)}{\sqrt{2\pi}\,\mathrm{erf}\,(x)}, \quad \alpha_2 = \frac{x \exp(-x^2)}{2\sqrt{\pi}\,\mathrm{erf}\,(x)} \tag{43}$$

where $x = \theta_w/(2\sigma_\theta)$. These functions are plotted in Fig. 4. Threshold value of q_0 is shown as well:

$$\frac{|q_0|_{thresh}}{Q_s} = \frac{1}{[1 + 2\alpha(x)]\,\mathrm{erf}\,(x)} \tag{44}$$

It is seen that shortening of the wake results in an increase of the threshold which becomes especially noticeable at $\theta_w <\sim 2\sigma$.

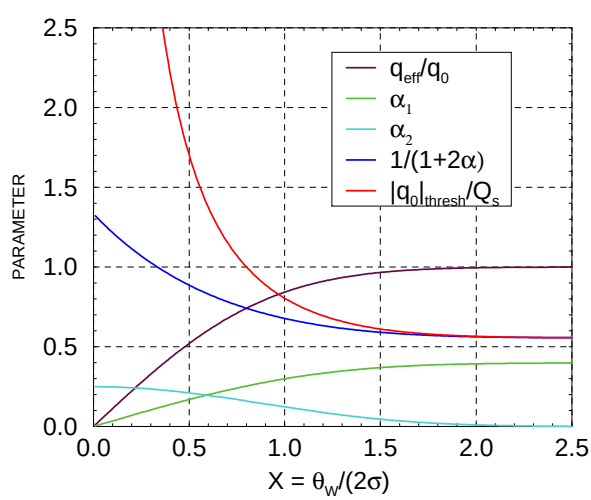

FIG. 4: Parameters of Gaussian bunch with short rectangular wake. Brown line describes an effective deterioration of the wake in a short bunch, red line represents TMCI threshold.

B. Resistive wake

Resistive wall impedance is the most general and important source of transverse instabilities in circular accelerators. Corresponding normalized wake function is

$$q(\theta) = \frac{q_0}{\sqrt{\theta}}, \qquad q_0 = -\frac{r_0 R^2 N}{2\pi\beta\gamma Q_0 b^3}\sqrt{\frac{c}{R\sigma_c}} \tag{45}$$

where b is the beam pipe radius, and σ_c is the pipe wall conductivity (see e.g. [7]). With this wake, integrals in Eq. (42) are representable in terms of gamma functions:

$$q_{ef} = \frac{q_0\,\Gamma(1/4)}{\sqrt{2\pi\sigma_\theta}} = \frac{1.4464\,q_0}{\sqrt{\sigma_\theta}}, \tag{46a}$$

$$\alpha_1 = \frac{\Gamma(3/4)}{\sqrt{2}\,\Gamma(1/4)} = 0.2390, \qquad \alpha_2 = \frac{1}{8} \tag{46b}$$

Threshold value of effective and usual wakes can be found then with help of Eq. (41): $|q_{ef}|_{thresh} = 0.739\,Q_s$, $|q_0|_{thresh} = 0.511\,Q_s\sqrt{\sigma_\theta}$. Therefore, with usual notation, the resistive wall TMCI threshold is

$$\frac{r_0 R^2 N_{thresh}}{2\pi\beta\gamma Q_0 Q_s b^3}\sqrt{\frac{c}{\sigma_c\sigma_z}} = 0.51 \tag{47}$$

where standard bunch length $\sigma_z = \sigma_\theta R$ is used. Note an essential decrease of the threshold at the bunch shortening which effect is explained by a concentration of the particles in the strong wake field area. Of course, it is necessary to take into account that Eq. (45) is valid only at $R\theta >\sim b/\gamma$ where the wake reaches a maximal value. Therefore sufficient condition of applicability of Eq. (47) can be written as $\sigma_z \gg b/\gamma$.

Another restriction comes from the fact that the resistive wake has a long and slowly decaying tail. Therefore it can reach not only neighboring bunches but also succeeding turns. These multibunch/multiturn collective effects should be included to a comprehensive investigation of resistive wall instabilities. However, this point is beyond the scope of this work where only single bunch effects are examined. Nevertheless obtained results give a possibility to estimate a relative danger of the transverse mode coupling and the collective instabilities.

The bunch population should be taken for this estimation as the threshold value given by Eq. (47). Then the TMCI tune shift is $|\nu|_{\rm TMCI} \simeq 0.77\,Q_s$ as it can be seen from Fig. 1-3. The collective modes tune shift with this intensity is [7]

$$|\nu|_{\rm COL} \simeq 0.51\,Q_s\sqrt{\frac{2\beta\sigma_z}{2\pi R|k-Q|}}\left(h - \frac{(2|k-Q_0|)^{3/2}}{h^{1/2}}\right) \tag{48}$$

where h is number of bunches, and k is the collective mode number (the mode can be unstable at $k > Q_0$). We accept further $|k - Q_0| = 0.25$ and $\beta = 1$ to estimate the maximal shift and to get the ratio:

$$\left|\frac{\nu_{\rm COL}}{\nu_{TMCI}}\right| \sim 2\left(h - \frac{0.35}{\sqrt{h}}\right)\sqrt{\frac{\sigma_z}{2\pi R}} \tag{49}$$

With great probability this value is < 1 or even $\ll 1$ at $h = 1$, that is the multiturn effect of single bunch is small or ever negligible in comparison with TMCI. However, the collective effects are more danger in a multibunch machine with $h \gg 1$, $h\sigma_z \sim R$. Of course, more detailed analysis is required at intermediate cases.

VII. TMCI WITH SPACE CHARGE

TMCI with ultimate space charge was considered in works [4-7]. The most remarkable effect is a pronounced asymmetry of the curves with respect to the wake sign as it has been shown in Ref. [6]. It is illustrated by Fig. 5 taken from quoted article where a rectangular ("boxcar") bunch with constant wake was explored at space charge betatron tune shift $\Delta Q_0 \gg Q_s$. It is seen that TMCI appears only with positive wake satisfying the instability condition

$$(q_0)_{thresh} \simeq \frac{0.5\, Q_s^2}{\Delta Q_0} \tag{50}$$

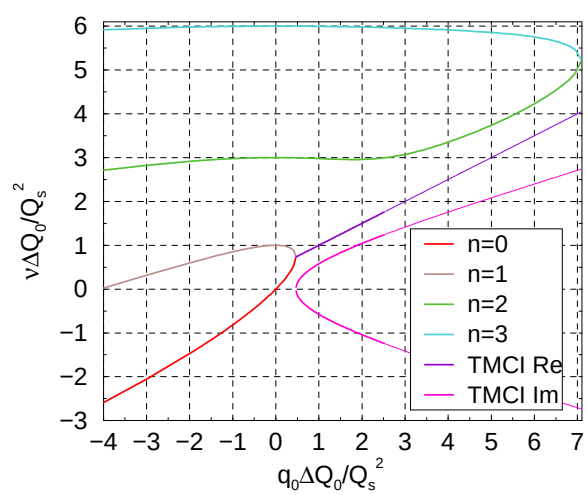

FIG. 5: TMCI with space charge by [6]. Boxcar bunch, $n = m(m+1)/2$.

which drastically differs from the conditions presented by Fig. 1-3 and Eq. (30) of this paper. It is needless to say that investigation of the effect at $\Delta Q_0 \sim Q_s$ is the only way to resolve the problem by a joining of these conflicting pictures. It turns out that just Eq. (32) bridges these ultimate cases providing a general form of the bunch eigenfunction near the TMCI threshold.

Actually, Eq. (8) has been presented in Ref. [6] just in the form with space charge included:

$$\nu Y + i\,Q_s \frac{\partial Y}{\partial \phi} + \Delta Q_{av}\left(\rho(\theta)Y(\theta,u) - \int_{-\infty}^{\infty} F(\theta,u)Y(\theta,u)du\right)$$
$$= 2q_0 \exp(i\zeta_\nu \theta)\int_{\theta}^{\infty} \exp(-i\zeta_\nu \theta')d\theta' \int_{-\infty}^{\infty} F(A')Y(A',\phi')\,du' \qquad (51)$$

with ΔQ_{av} as the space charge tune shift averaged on all coordinates. We will consider further a rectangular bunch where tune shift does not depend on θ; then $\rho = 1/2$ and $Q_{av} = Q_0$. Thereupon, using Eq. (32) as a pattern of the solution, one can get the expression like Eq. (33) with the only addition $\Delta Q_0 C_u u$ in the left hand part. Therefore relation between coefficients obtains the form $C_u = iC_\theta Q_s/(\nu + \Delta Q_0)$ resulting in the dispersion equation (without chromaticity)

$$\frac{\nu - q_0}{2}\left(\nu - \frac{Q_s^2}{\nu + \Delta Q_0}\right) = -\alpha^2 q_0^2 \qquad (52)$$

It looks like Eq. (25) but can have rather different solutions dependent on the parameter $\Delta Q_0/Q_s$. Some of them are plotted in Fig. 6 which displays the asymmetry very clearly: space charge propels the TMCI threshold to the centerline at $q_0 > 0$, and away from it at $q_0 < 0$. Corresponding dependence is shown quantitatively in Fig. 7 being presented separately for positive and negative wakes and supplemented by appropriate analytical formulae. There is very good agreement of these results with Fig. 5. For example, TMCI threshold of positive wake is

$$(q_0)_{thresh} = \frac{0.57\,Q_s^2}{Q_s + \Delta Q_0} \to \frac{0.57\,Q_s^2}{\Delta Q_0}$$

what is very close to the estimation given by Eq. (50).

However, it is well to bear in mind that more often than not wakes have negative sign in reality. Space charge tune shift raises the TMCI threshold in such a case, and in this sense it promotes the beam stability. For example, Eq. (47) for resistive wall TMCI threshold obtains the form

$$\frac{r_0 R^2 N_{thresh}}{2\pi\beta\gamma Q_0 Q_s b^3}\sqrt{\frac{\Omega_0 R}{\sigma_c \sigma_z}} \simeq 0.51\left(1 + \frac{0.7\Delta Q_0}{Q_s} + \frac{0.3\Delta Q_0^2}{Q_s^2}\right)$$

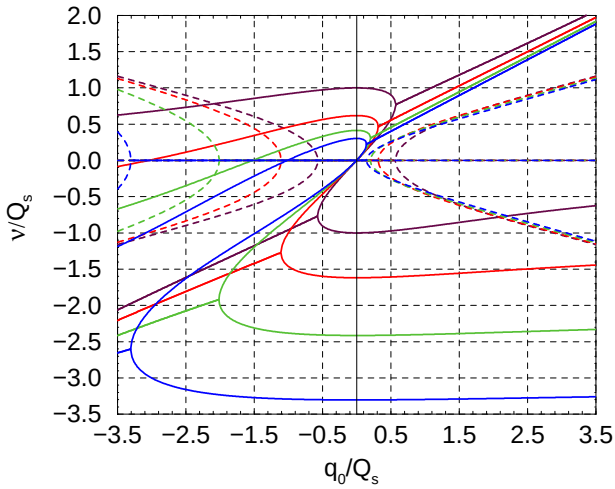

FIG. 6: TMCI of rectangular bunch without chromaticity but with space charge. Presented ratios $\Delta Q_0/Q_s$ are: 0 (maroon), 1 (red), 2 (green), and 3 (blue). Solid/dashed lines relate to real/imaginary parts of the tune.

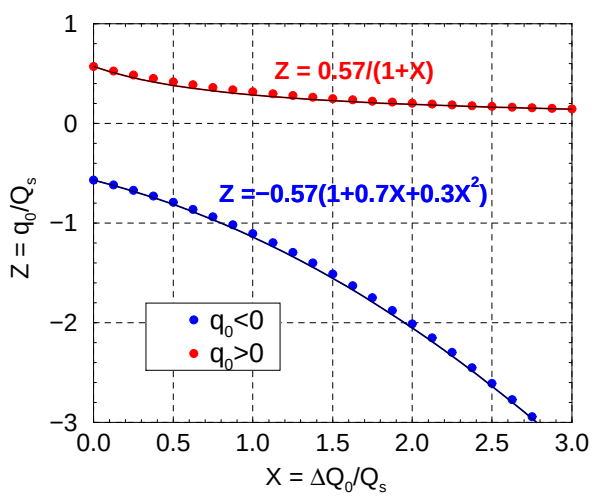

FIG. 7: TMCI threshold of the rectangular bunch against the space charge tune shift. Positive and negative wakes are presented separately, no chromaticity.

VIII. SUMMARY

Theory of transverse mode coupling instability is proceeded in the paper being founded on exact solution of equations for hollow bunch, and on three-modes approximation for

arbitrary one.

It is shown without additional assumptions that different TMCI modes of the hollow bunch arise through a coalescence of 2 neighboring multipoles which frequencies approach each other under the influence of wake field. The multipoles of indexes $m = (0-1),\ (2-3)$ etc. are coalescing to create first, second, etc. TMCI modes if the wake is positive, and the same happens with negative multipoles at negative wake. There were no other kinds of the TMCI appearances observed at these calculations.

The lowest TMCI mode arises by coalescing of multipoles $m = 0$ and $m = \pm 1$ dependent on sign of the wake. It holds the greatest interest in practice because all other TMCI modes have significantly higher thresholds of intensity. Therefore this mode is investigated in detail in the paper.

Special 3-modes approach is developed to be applied to arbitrary shaped bunch. The method allows to get very simple 3-order dispersion equation for the bunch eigentunes which has 3 different solutions at given wake strength. For hollow bunch, these solutions coincide very closely with mentioned exact results having a difference certainly less of 0.1%.

Another interesting point obtained by this method is very slight dependence of the instability parameters on the bunch shape. For example, difference of the TMCI thresholds is less of 1% even for so variously shaped bunches as hollow and Gaussian ones, if they have the same rms length.

A modest modification of this method allows to take into account effects of chromaticity. TMCI has no clear threshold in this case because this kind of instability grows more or less smoothly from the head-tail instability owing to coalescence of the lowest radial modes of low-order multipoles. Higher radial modes do not contribute to this process because their coalesce would require significantly higher intensity. Dependence of the instability rate on bunch shape remains at the level of several percents if the bunches rms length is fixed.

The results obtained with a simple constant wake are extended in the paper to arbitrary wakes. In particular, dependence of TMCI on the length of rectangular wake is investigated thoroughly demonstrating that its threshold increases significantly when the wake becomes shorter than 2σ of the bunch.

More complicated results are obtained with resistive wall wake. It is shown that corresponding TMCI effect significantly increases at the bunch shortening, so it can easy overpower well known effect of single bunch multiturn instability. However, the collective insta-

bility can prevail in multibunch machine though special analysis is needed in each concrete case. Simple formula for comparison is presented in the paper.

Space charge is included in consideration at the end of the paper to make a bridge between the known ultimate cases of neglected space charge tune shift and dominating one. It is confirmed that space charge decreases threshold of positive wakes and increases it if the wake is negative. Simple analytical formulae are proposed in both cases to describe dependence of the threshold on the tune shift.

Taking into account that wake field is negative more often than not, one can say that TMCI is typically depressed by the space charge.

---

[1] R. Kohaupt, in *Proceeding of the XI International Conference on High Energy Accelerators, p. 562, Geneva (1980).*

[2] V.V. Danilov and E.A.Perevedentsev, Nucl. Instrum. Metods Phys. Res., Sect. A 391, 77 (1977).

[3] V.V. Danilov, Phys. Rev. ST Accel. Beams 1,041301 (1998).

[4] M. Blaskiewicz, Phys. Rev. ST Accel. Beams 1,044201 (1998).

[5] A. Burov, Phys. Rev. ST Accel. Beams 12,044202 (2009).

[6] V. Balbekov, Phys. Rev. ST Accel. Beams 14,094401 (2011).

[7] V. Balbekov, Phys. Rev. ST Accel. Beams 15,054403 (2012).

IX. APPENDIX: DERIVATION OF EQ. (28)

With $Y_0 = 1$, it follows from Eq. (24) and (27)

$$\alpha^2 = 8\pi^3 \int_0^\infty F(A)\, A dA \left[\int_0^\infty K_{0,1}(A', A) F(A') A'\, dA' \right]^2$$

Substitution of $K_{0,1}$ from Eq. (21) results in

$$\alpha^2 = \frac{128}{\pi} \int_0^\infty F(A) \frac{dA}{A} \left[\int_0^\infty F(A') A' dA' \int_0^{A'} \sqrt{\frac{A^2 - \theta_A^2}{A'^2 - \theta^2}}\, d\theta \right]^2$$

where $\theta_A = \theta$ or A. Changing sequence of the integrals obtain

$$\alpha^2 = \frac{128}{\pi} \int_0^\infty F(A) \frac{dA}{A} \left[\int_0^A \sqrt{A^2 - \theta^2}\, d\theta \int_\theta^\infty \frac{F(A') A'\, dA'}{\sqrt{A'^2 - \theta^2}} \right]^2$$

The last integral is $\rho(\theta)/2$ so the expression is reducible in the form

$$\alpha^2 = \frac{8}{\pi} \int_0^\infty F(A) A^3 \, dA \left[\int_{-1}^{1} \rho(A\xi) \sqrt{1-\xi^2} \, d\xi \right]^2$$

which can be transformed in Eq. (28) by the substitution $\xi = \cos\phi$.